Diffusion Tensor Fiber Tracking Shows Distinct Corticostriatal Circuits in Humans

Stéphane Lehéricy, MD, PhD,[1,2,5] Mathieu Ducros, PhD,[7] Pierre-François Van de Moortele, MD, PhD,[1] Chantal Francois, PhD,[4] Lionel Thivard, MD,[3] Cyril Poupon, PhD,[5] Nick Swindale, PhD,[6] Kamil Ugurbil, PhD,[1] and Dae-Shik Kim, PhD[1]

A landmark of corticostriatal connectivity in nonhuman primates is that cortical connections are organized into a set of discrete circuits. Each circuit is assumed to perform distinct behavioral functions. In animals, most connectivity studies are performed using invasive tracing methods, which are nonapplicable in humans. To test the proposal that corticostriatal connections are organized as multiple circuits in humans, we used diffusion tensor imaging axonal tracking, a new magnetic resonance technique that allows demonstration of fiber tracts in a noninvasive manner. Diffusion tensor imaging–based fiber tracking showed that the posterior (sensorimotor), anterior (associative), and ventral (limbic) compartments of the human striatum have specific connections with the cortex, and particularly the frontal lobes. These results provide the first direct demonstration of distinct corticostriatal connections in humans.

Ann Neurol 2004;55:522–529

Over the past 15 years, anatomical studies in animals have shown that all cortical areas project to the striatum in discrete circuits.[1] These circuits are subdivided into subchannels conveying either sensorimotor, association, or limbic information.[1] Most fiber tract studies in animals rely on invasive techniques, which are not applicable to human studies. To date, the hypothesis initially proposed by Alexander and colleagues[1] that corticostriatal connections are organized in discrete channels has not been tested in humans, and the corticobasal ganglia connectivity is largely based on primate–human extrapolations.

Diffusion tensor imaging (DTI) is a new technique that allows demonstration of fiber tracts in vivo in humans.[2–4] In the white matter, water diffusion is directionally dependent, a property called anisotropy. Diffusion in the white matter is higher following the direction of fiber bundles, which is attributed to the organization of axons and myelin sheaths. Using DTI and fiber tracking algorithms, previous studies have shown reconstruction of well-known fiber tracts.[5,6] Fiber tracking has been validated in postmortem animal studies.[7] Evidence that DTI-based fiber tracking has the ability to provide new insight on the organization of human fiber tracts anatomy is still awaited, however. In this study, we used DTI imaging and axonal tracking to parcel out the anatomical connections of the human striatum.

Subjects and Methods

Subjects

Nine healthy right-handed volunteers were studied (three men, six women; age range,24–33 years). The National Ethics Committee approved the study. All subjects gave informed consent.

Imaging

DTI was performed using echo planar imaging (EPI) at 1.5T (GE) with standard head coil for signal reception. DTI axial slices were obtained using the following parameters: TR, 10 seconds; TE, 88 milliseconds; flip angle, 90 degrees; matrix, 128 × 128; field of view, 380 × 380mm^2; slice thickness, 3mm no gap (3mm isotropic voxels), four excitations; acquisition time [5 minutes 20 seconds]. Diffusion weighting was performed along six independent directions, with *b*-value of

From the [1]Center for Magnetic Resonance Research, University of Minnesota Medical School, Minneapolis, MN; [2]Department of Neuroradiology, CHU Salpètrière, [3]Laboratoire de Neurophysiologie et Nouvelles Microscopies ESPCI-INSERM EPI 00-02, [4]Inserm U289, and [5]Department of Neurology, CHU Salpetrière, Paris; and [6]Service Hospitalier Frédéric Joliot, CEA, Orsay, France; [7]Department of Ophthalmology and Visual Sciences, University of British Columbia, Vancouver, Canada; [8]Department of Anatomy and Neurobiology, Boston University School of Medicine, Boston, MA

Received Jul 28, 2003, and in revised form Nov 1. Accepted for publication Dec 1, 2003.

Published online Mar 22, 2004, in Wiley InterScience (www.interscience.wiley.com). DOI: 10.1002/ana.20030

Address correspondence to Dr Lehéricy, CMRR, 2021 6th Street SE, Minneapolis, MN 55455. E-mail: lehericy@cmrr.umn.edu

900sec/mm^2. A reference image with no diffusion weighting was also obtained. High-resolution three-dimensional anatomical images were used for display.

Image Processing

Raw diffusion-weighted data were corrected for geometric distortion secondary to eddy currents using a registration technique based on the geometric model of distortions.[8] Diffusion tensors, fractional anisotropy (FA), and fiber tracts were calculated using in-house software. The fiber tracking algorithm used is based on the method described in Basser and colleagues.[2] Fiber tracts were propagated along the direction of the eigenvector associated with the greatest eigenvalue over a small distance (<1mm) to the next point where a new diffusion tensor was interpolated. Fiber tracking terminated when the angle between two consecutive eigenvectors was greater than 60 degrees, or when the FA value was smaller than 0.1, indicating a region of low diffusion anisotropy. A spherical shape marker indicated the fiber termination points.

Anatomical Localization of Fibers

The anatomical localization of fiber end points in the frontal lobes was first performed on high-resolution three-dimensional T1-weighted images. Coregistration was performed by matching reproducible landmarks (such as the hand area, the anterior commissure, the corpus callosum) between the two types of images. The frontal lobes were divided anatomically into several subsectors. The motor cortex included the cortex anterior to the central sulcus and posterior to the precentral sulcus. The premotor cortex included the cortex anterior to the precentral sulcus and posterior to an oblique line linking the lower part of the precentral sulcus to the brain vertex at the level of the ventral commissure anterior (VCA) line, a vertical line that intersects the anterior commissure and that is perpendicular to the anterior commissure-posterior commissure plane. The supplementary motor area (SMA) and the pre-SMA were located in the medial frontal wall, caudal and rostral to the VCA line, respectively. The prefrontal cortex corresponded to the lateral surface of the frontal lobe, rostral to the premotor cortex, and was subdivided in the dorsolateral prefrontal cortex (defined as the prefrontal cortex dorsal to the inferior frontal sulcus) and the ventrolateral frontal cortex (ventral to the inferior frontal sulcus including the lateral orbitofrontal cortex). The medial orbitofrontal cortex included the orbital and medial frontal gyri. Anatomical and DTI images then were normalized to Talairach coordinates (SPM99; Wellcome Department of Cognitive Neurology, London) to determine the Brodmann area (BA) location of cortical connections.

Anatomical Definitions of the Seeding Points in the Basal Ganglia

Tracking was initiated from four regions of interest (ROIs) defined three-dimensionally in each hemisphere and located at reproducible anatomical positions. The ROI in the posterior putamen (Fig 1A, red) was located close to the dorsal

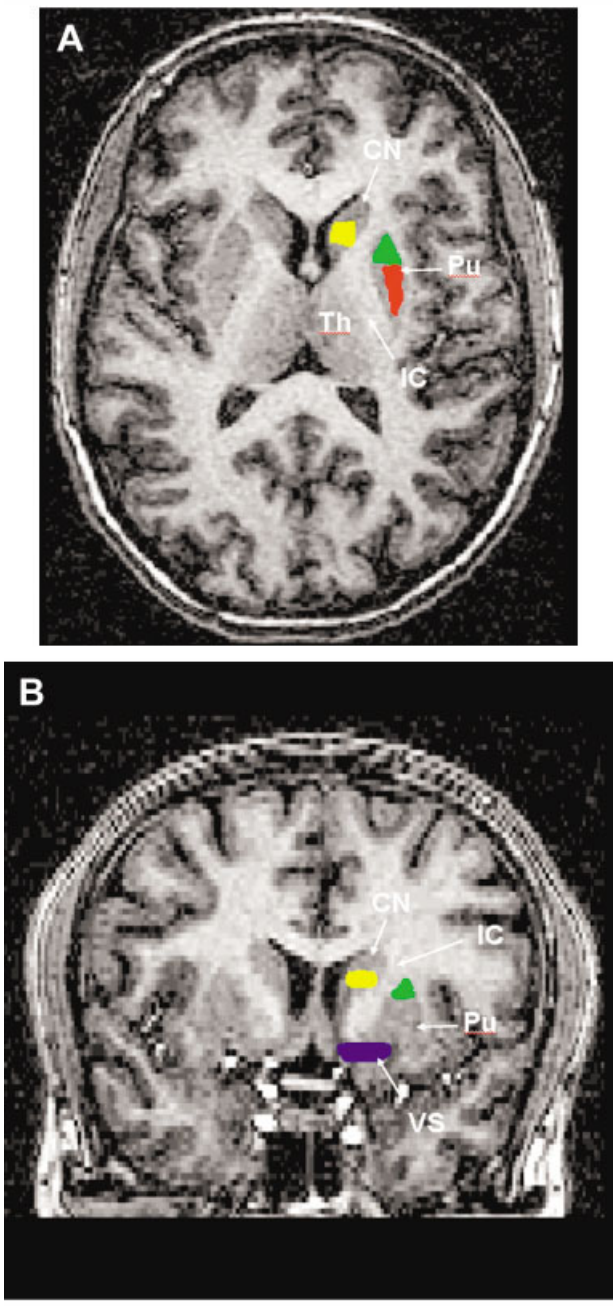

Fig 1. Location of the four regions of interest (ROIs). (A) Axial T1-weighted image passing at the level of the upper part of the putamen and (B) coronal T1-weighted image passing at the level of the rostral part of the striatum showing the location of the ROIs. The posterior putamen is represented in red, the anterior putamen in green, the caudate nucleus in yellow, and the ventral striatum in blue. Left is right. IC = internal capsule; CN = caudate nucleus; Pu = putamen; Th = thalamus; VS = ventral striatum.

border of the putamen caudal to the VCA line of Talairach (mean ROI volume ± SD: 420 ± 92; left, 474 ± 139mm^3 in the right and the left hemispheres, respectively). The ROI in the anterior putamen (see Fig 1A, B, green) was located rostral to the VCA line (right, 432 ± 121; left, 413 ±

126mm^3). The ROI in the caudate nucleus (see Fig 1A, 1B, yellow) was located in the gray matter of the dorsal part of the nucleus, adjacent to the anterior part of the internal capsule (477 ± 95; left, 450 ± 109mm^3). The ROI in the ventral striatum (see Fig 1B, blue) was traced on coronal views in the anterior part of the striatum inferior to the internal capsule (right, 378 ± 38; left, 365 ± 57mm^3). ROI volumes were not different between the right and the left hemispheres.

Results

Fibers originating from the posterior striatum were found in the corona radiata, directed toward the motor and adjacent premotor cortex (BA 4, 18 of 18 hemispheres), the primary sensory cortex (BA 1, 2, 3, 16 hemispheres), the posterior part of the SMA (BA 6, 18 hemispheres), and the mesencephalon (15 hemispheres; Figs 2A and 3). Striatomesencephalic fibers formed a discrete bundle, which ended in the medial part of the cerebral peduncle and the substantia nigra (see Fig 3).

For the anterior putamen, fiber tracts were located into the anterior part of the corona radiata toward the anterior medial (pre-SMA, 16 hemispheres) and lateral premotor cortex (BA 6 and 8) and the prefrontal cortex (see Fig 2B). In the prefrontal cortex, end points of fibers were observed in the ventrolateral (eight hemispheres, BA 45 and 47) and dorsolateral prefrontal cortex (14 hemispheres, BA 9 and 46). Fibers directed to the mesencephalon were observed in seven hemispheres. Fiber tracts associated with the head of the caudate nucleus (see Fig 2B) were directed toward the medial prefrontal cortex (rostral to pre-SMA, 9 hemispheres), the dorsal (BA 9 and 46) and ventral (BA 45 and 47) prefrontal cortex (10 and 7 hemispheres, respectively), the frontal pole (BA 10, 13 hemispheres), and the mesencephalon (11 hemispheres). Overall,

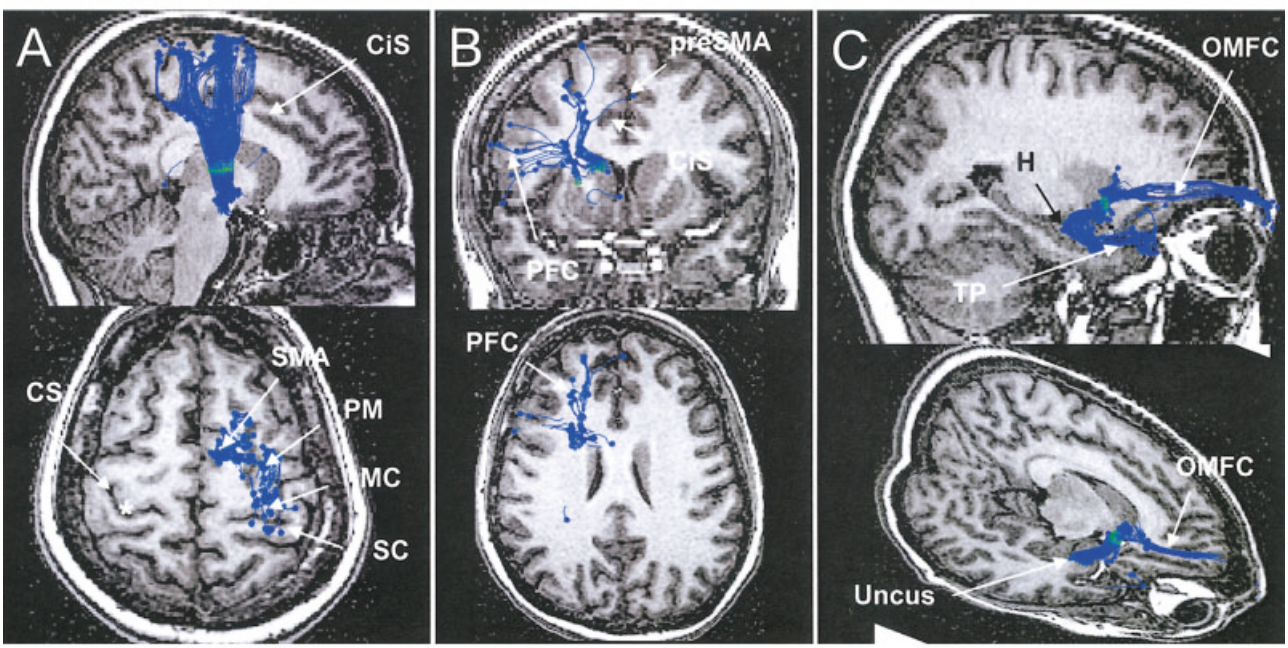

Fig 2. Corticostriatal tract reconstructions. Fiber tracts are represented on T1-weighted sections. (A) Tracking results for the posterior putamen (the region of interest is represented in green). The blue fibers represent the tract in three dimensions as if viewed from the right and projected on a parasagittal slice (up) or from the top of the brain and projected on an axial slice (down). Fiber tracts (blue) were located in the corona radiata and ended in the motor and adjacent premotor cortex, the primary sensory cortex, the supplementary motor area (SMA), and the mesencephalon. (B) Tracking results for the anterior striatum. The blue fibers represent the tract in three dimensions as if viewed from the front and projected on a coronal view (up) or from the top of the brain and projected on an axial slice (down). ROIs (green) were located in the anterior putamen and the head of the caudate nucleus. Fiber tracts were located into the anterior corona radiata toward the pre-SMA, the prefrontal cortex, and the frontal pole. (C) Tracking results for the ventral striatum. The blue fibers represent the tract in three dimensions as if viewed from the right and projected on a parasagittal slice (up) or from the anterior-right of the brain and projected on a three-dimensional view (down). Fiber tracts were directed toward the medial orbitofrontal cortex, the uncus of the temporal lobe, and the temporal pole. CS = central sulcus; CiS = cingulate sulcus; H = hippocampus; MC = motor cortex; OMFC = orbitomedial frontal cortex; PFC = prefrontal cortex; PM = premotor cortex; SC = primary sensory cortex; SMA = supplementary motor area; TP = temporal pole. Asterisk indicates the hand motor area (hand knob).

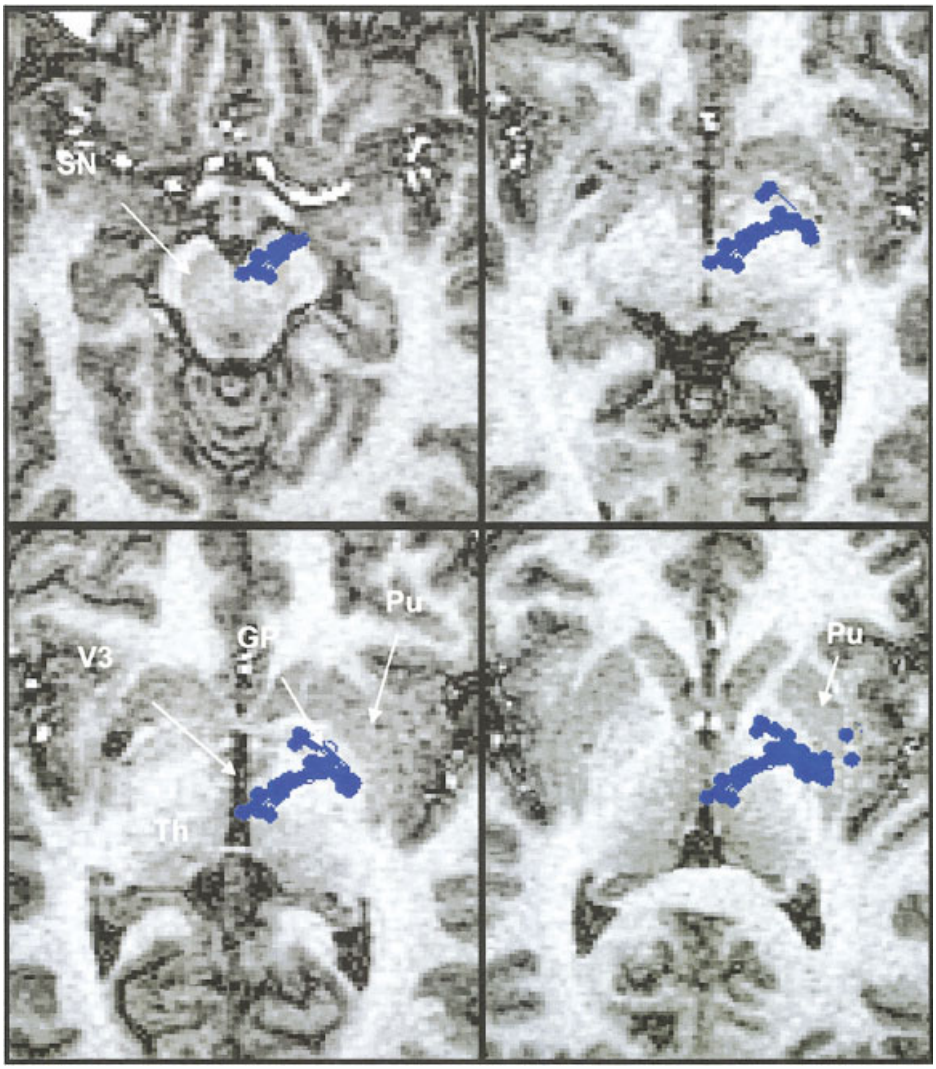

Fig 3. Striatomesencephalic fibers. Four axial T1-weighted images passing at the level of the mesencephalon (upper left), the subthalamic area (upper right), and the thalamus (lower left and right). The blue fibers represent the tract in three dimensions as if viewed from below the slice. Fibers coursed from the putamen through the globus pallidus, reached the subthalamic area, and converged to the medial part of the substantia nigra. GP = globus pallidus; Pu = putamen; SN = substantia nigra; Th = thalamus; V3 = third ventricle.

these frontal fibers were rostral to those coming from the anterior putamen.

For the ventral striatum, fiber tracts were directed toward the medial orbitofrontal cortex (MOFC, BA 11, 32 and 25, 18 hemispheres), the ventromedial frontal pole (8 hemispheres, BA 10, 12 hemispheres), the uncus of the temporal lobe (18 hemispheres, BA 38), and the temporal pole (6 hemispheres; see Fig 2C). Fibers to the uncus of the temporal lobe were located ventral to the putamen–pallidum complex, in the substantia innominata. Other connections were not consistent, observed in four hemispheres or less.

Tracking then was initiated from cortical areas. Cortical ROIs included the motor, premotor, prefrontal, and orbitomedial frontal cortex (see Subjects and Methods). Figure 4 displays interindividual variability of the results in the left hemisphere of all subjects. Fibers originating from the motor cortex were directed to the posterior part of the putamen. Premotor fibers were rostral to motor fibers although overlapping with these fibers. Fibers originating from the prefrontal cortex occupied most of the anterior striatum and the head of the caudate nucleus. Results were more variable in the anterior striatum, such as for Subject 6. Fibers originating from the orbitomedial frontal cortex were directed to the ventral striatum.

The relationships of these fibers with adjacent fiber bundles also were determined (Fig 5). Large ROIs were also traced in the posterior (see Fig 5A) and anterior (see Fig 5B) parts of the internal capsule in six hemispheres. Striatal fibers were distinct from those passing through the internal capsule in all six hemispheres. End points of the fibers merged in the cortex and the corona radiata but were distinct in the lower part of the corona radiata and once reaching the striatum. Striatomesencephalic fibers and corticospinal fibers passing through the internal capsule remained separate. At striatal level, striatomesencephalic fibers were located laterally to those of the corticospinal tract. At mesence-

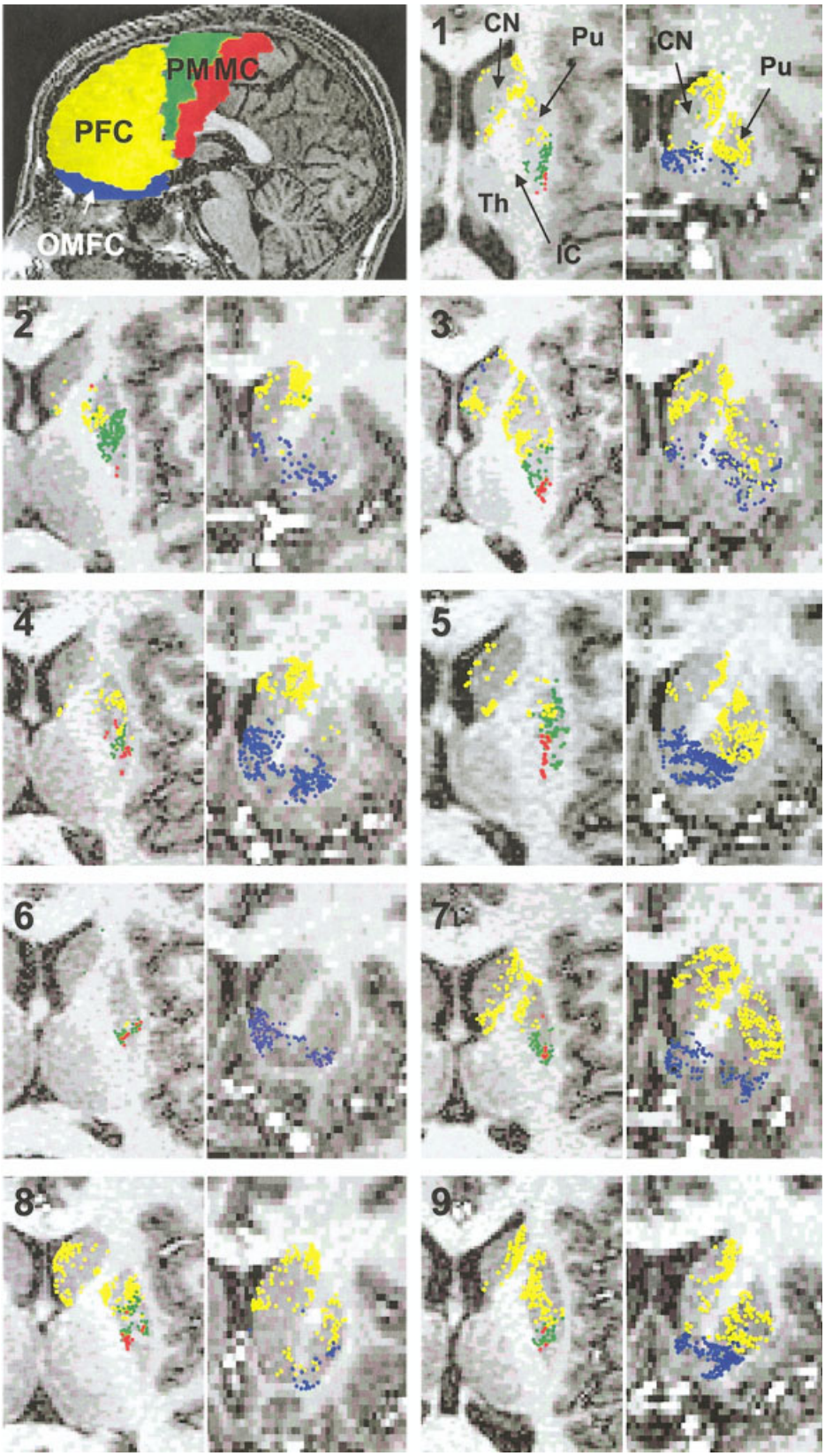

Fig 4. Connectivity maps of the striatum. (A) Tracking was initiated from four regions of interest located in the frontal lobes, including the motor (red), premotor (green), prefrontal (yellow), and orbitomedial frontal cortex (blue) in the left hemisphere of all subjects. Only fibers crossing the striatum are displayed in the axial (left) and coronal (right) planes as a small dot superimposed on T1-weighted anatomical images. Fibers originating from the motor cortex were directed to the posterior part of the putamen (red). Premotor fibers were rostral to motor fibers although overlapping with these fibers (green). Fibers originating from the prefrontal cortex occupied most of the anterior striatum and the head of the caudate nucleus (yellow). Fibers originating from the orbitomedial frontal cortex were directed to the ventral striatum (blue). Variable overlap existed between the different striatal territories. CN =caudate nucleus; IC = internal capsule; MC = motor cortex; OMFC = orbitomedial frontal cortex; PFC = prefrontal cortex; PM = premotor cortex; Pu = putamen; Th = thalamus.

phalic level, these fibers were rostral and medial to the corticospinal tract.

Discussion

Our findings provide the first anatomical evidence that corticostriatal connections in humans are organized into discrete circuits, similar to the organization described with tracing studies in monkeys. The results showed that each striatal compartment has specific connections with the cortex, and particularly the frontal lobes. They also show connections to the mesencephalon probably corresponding to striatonigral and nigrostriatal fibers.

The sensorimotor compartment of the putamen (posterior part of the putamen) was connected to the primary sensory and motor areas and to the posterior part of the SMA. In monkeys, the sensorimotor cortex and the SMA project mainly toward the dorsal part of the postcommissural portion of the putamen.[9–11] Corticostriatal and corticospinal fibers passing through the posterior part of the internal capsule originated from the same brain areas but separated in the lower part of the corona radiata. Striatomesencephalic fibers remained separated from corticospinal fibers at all subcortical levels. These fibers most probably correspond to striatonigral fibers which are myelinated and to nigrostriatal dopaminergic fibers. In animals, nigrostriatal fibers originate from the dorsal part of the substantia nigra, course dorsal to the subthalamic nucleus then ascend laterally to the globus pallidus.[12] Striatonigral fibers follow the same course.[13] This trajectory is highly consistent with the one observed here. Positron emission tomography and functional magnetic resonance imaging studies have shown that the sensorimotor compartment of the pu-

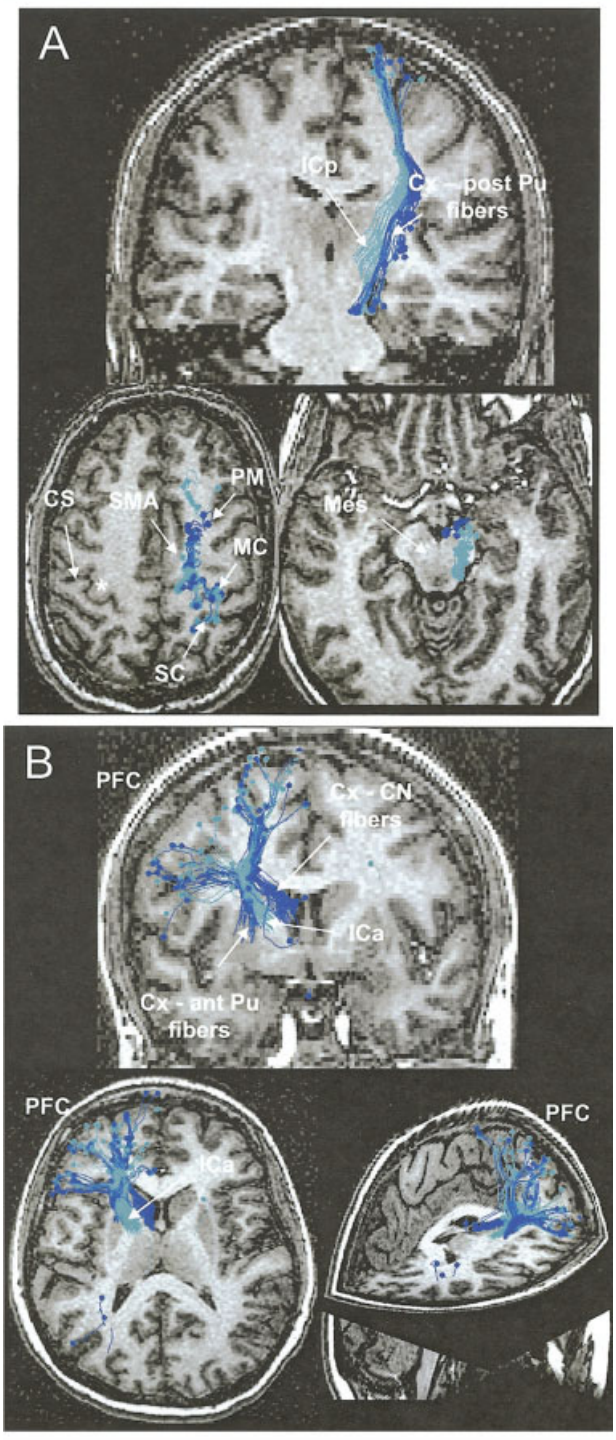

Fig 5. Comparison of corticostriatal fibers and cortical fibers passing through the internal capsule. Fiber tracts are represented on T1-weighted sections. (A) Corticostriatal (dark blue) and corticospinal fibers passing through the posterior part of the internal capsule (light blue). The fibers represent the tract in three dimensions as if viewed from the front and superimposed on coronal view (up), from above an axial slice passing at the level of the motor cortex (lower left) or from below an axial slice passing at the level of the mesencephalon (lower right). The two bundles originated from the same brain areas (lower left) but separated in the lower part of the corona radiata close to the upper border of the putamen. Striatomesencephalic fibers remained separated from corticospinal fibers at all subcortical levels (lower right). (B) Corticostriatal fibers (dark blue) and cortical fibers passing through the anterior part of internal capsule (light blue). The fibers represent the tract in three dimensions superimposed on a coronal slice as if viewed from the front (up), an axial slice as if viewed from above (lower left), or from the posterior-right of the brain and projected on a three-dimensional view (lower right). The two bundles originated from the same brain areas and separated in the lower part of the corona. ant = anterior; CS = central sulcus; Cx = cortex; ICa = anterior part of the internal capsule; ICp = posterior part of the internal capsule; MC = motor cortex; Mes = mesencephalon; PFC = prefrontal cortex; PM = premotor cortex; post = posterior; SC = primary sensory cortex; SMA = supplementary motor area. Asterisk indicates the hand motor area (hand knob).

tamen has a primary executive role in the control of movement.[14,15]

The associative compartment of the striatum (anterior striatum) was connected to the prefrontal cortex, the frontal pole, and the pre-SMA. In monkeys, pre-SMA projections are predominantly directed to the anterior part of the caudate nucleus and putamen,[11,16–19] in striatal regions located rostral to SMA projections to the striatum.[18] In line with these observations,[18] pre-SMA connections to the striatum were observed twice as frequently for ROIs in the anterior putamen than in the head of the caudate nucleus. In monkeys, the dorsolateral prefrontal cortex territory occupies a central position within the anterior striatum predominating in the caudate nucleus, whereas the ventrolateral prefrontal cortex territory is more medially and ventrally located.[16,19] The frontal pole projects mainly to the head of the caudate nucleus,[16,19] in line with our results. In monkeys, temporal and parietal areas also project to the anterior striatum.[20,21] In our subjects, connections of temporal and parietal areas with the basal ganglia were rarely observed, and when present directed to the anterior striatum. This is in line with the fact that projections from these areas are less dense than those originating from the frontal cortex. Functional imaging studies in humans have shown that the anterior striatum was activated during more complex motor tasks than the posterior putamen.[14,22,23]

The limbic compartment of the striatum (ventral striatum) had highly reproducible connections across subjects. Tracing studies in monkeys have shown that the ventral striatum receives afferents from structures associated with the limbic system,[24] including the orbitomedial frontal cortex,[25] the amygdala,[26–28] the hippocampus,[28] the anterior cingulate cortex,[29] and the temporal pole.[20] As in this study, amygdala afferents to the ventral striatum courses through the substantia innominata and the nucleus basalis of Meynert.[26] Except for the anterior cingulate cortex, these data are in agreement with our results. In nonhuman primates, many striatal neurons respond to reward or anticipation of reward and use that information to build goal-directed behavior.[30] Several functional magnetic resonance imaging studies have reported activation in the ventral striatum and ventral or medial frontal regions during monetary reward or punishment[31] and expectation of monetary reward.[32]

Limitations of fiber tracking also were observed, however. Connections with regions known to project to the striatum, such as the cingulate cortex-ventral striatal connections, were rarely observed. Moreover, tracking variability was observed across subjects, mostly in the anterior striatum (see Fig 4). These differences with animal studies likely result from the complexity of fiber directions in the anterior frontal lobe. Fiber direction estimated with DTI is the average of all fiber directions within each voxel. When fiber tracts cross or merge within one voxel, then the eigenvector associated with the largest eigenvalue of the diffusion tensor corresponds to the average of all directions in the voxel. Visual analysis of eigenvector maps showed kissing or crossing of fibers coming from the prefrontal cortex and directed to the anterior putamen and caudate nucleus occurred at this level probably limiting fiber tract reconstruction (see Fig 4, Subject 6). Increased spatial resolution or improved fiber tracking method may help overcome this limitation. Other possible sources of artifacts were B0-related EPI distortion, which resulted in a small upper displacement of connections between the orbitofrontal cortex and the ventral striatum. EPI distortion due to eddy currents and DTI-anatomical image coregistration were minimized as much as possible.

This study was supported by grants from the NIH (National Center for Research Resources, BTRR P41-RR008079, K.U.), the Keck Foundation, the Human Frontiers Science Program (K.U., D.S.K.), and the Inciting Joint Actions Committee (Actions Concertèes Incitatives, AC1-6503H, S.L.).

References

1. Alexander GE, DeLong MR, Strick PL. Parallel organization of functionally segregated circuits linking basal ganglia and cortex. Annu Rev Neurosci 1986;9:357–381.
2. Basser PJ, Pajevic S, Pierpaoli C, et al. In vivo fiber tractography using DT-MRI data. Magn Reson Med 2000;44: 625–632.
3. Mori S, Crain BJ, Chacko VP, van Zijl PC. Three-dimensional tracking of axonal projections in the brain by magnetic resonance imaging. Ann Neurol 1999;45:265–269.
4. Poupon C, Clark CA, Frouin V, et al. Regularization of diffusion-based direction maps for the tracking of brain white matter fascicles. Neuroimage 2000;12:184–195.
5. Mori S, Kaufmann WE, Davatzikos C, et al. Imaging cortical association tracts in the human brain using diffusion-tensor-based axonal tracking. Magn Reson Med 2002;47:215–223.
6. Stieltjes B, Kaufmann WE, van Zijl PC, et al. Diffusion tensor imaging and axonal tracking in the human brainstem. Neuroimage 2001;14:723–735.
7. Holmes AA, Scollan DF, Winslow RL. Direct histological validation of diffusion tensor MRI in formaldehyde-fixed myocardium. Magn Reson Med 2000;44:157–161.
8. Mangin JF, Poupon C, Clark C, et al. Distortion correction and robust tensor estimation for MR diffusion imaging. Med Image Anal 2002;6:191–198.
9. Kunzle H. Bilateral projections from precentral motor cortex to the putamen and other parts of the basal ganglia. An autoradiographic study in *Macaca fascicularis*. Brain Res 1975;88: 195–209.
10. Flaherty AW, Graybiel AM. Two input systems for body representations in the primate striatal matrix: experimental evidence in the squirrel monkey. J Neurosci 1993;13:1120–1137.
11. Middleton FA, Strick PL. Basal ganglia and cerebellar loops: motor and cognitive circuits. Brain Res Brain Res Rev 2000; 31:236–250.

12. Lavoie B, Smith Y, Parent A. Dopaminergic innervation of the basal ganglia in the squirrel monkey as revealed by tyrosine hydroxylase immunohistochemistry. J Comp Neurol 1989;289: 36–52.
13. Hedreen JC, DeLong MR. Organization of striatopallidal, striatonigral, and nigrostriatal projections in the macaque. J Comp Neurol 1991;304:569–595.
14. Jueptner M, Frith CD, Brooks DJ, et al. Anatomy of motor learning. II. Subcortical structures and learning by trial and error. J Neurophysiol 1997;77:1325–1337.
15. Lehericy S, van de Moortele PF, Lobel E, et al. Somatotopical organization of striatal activation during finger and toe movement: a 3-T functional magnetic resonance imaging study. Ann Neurol 1998;44:398–404.
16. Selemon LD, Goldman-Rakic PS. Longitudinal topography and interdigitation of corticostriatal projections in the rhesus monkey. J Neurosci 1985;5:776–794.
17. Brotchie P, Iansek R, Horne M. A neural network model of neural activity in the monkey globus pallidus. Neurosci Lett 1991;131:33–36.
18. Inase M, Tokuno H, Nambu A, et al. Corticostriatal and corticosubthalamic input zones from the presupplementary motor area in the macaque monkey: comparison with the input zones from the supplementary motor area. Brain Res 1999;833: 191–201.
19. Yeterian EH, Pandya DN. Prefrontostriatal connections in relation to cortical architectonic organization in rhesus monkeys. J Comp Neurol 1991;312:43–67.
20. Yeterian EH, Pandya DN. Corticostriatal connections of the superior temporal region in rhesus monkeys. J Comp Neurol 1998;399:384–402.
21. Cavada C, Goldman-Rakic PS. Posterior parietal cortex in rhesus monkey. II. Evidence for segregated corticocortical networks linking sensory and limbic areas with the frontal lobe. J Comp Neurol 1989;287:422–445.
22. Deiber MP, Passingham RE, Colebatch JG, et al. Cortical areas and the selection of movement: a study with positron emission tomography. Exp Brain Res 1991;84:393–402.
23. Baker SC, Rogers RD, Owen AM, et al. Neural systems engaged by planning: a PET study of the Tower of London task. Neuropsychologia 1996;34:515–526.
24. Alheid GF, Heimer L. New perspectives in basal forebrain organization of special relevance for neuropsychiatric disorders: the striatopallidal, amygdaloid, and corticopetal components of substantia innominata. Neuroscience 1988;27:1–39.
25. Haber SN, Kunishio K, Mizobuchi M, Lynd-Balta E. The orbital and medial prefrontal circuit through the primate basal ganglia. J Neurosci 1995;15:4851–4867.
26. Russchen FT, Bakst I, Amaral DG, Price JL. The amygdalostriatal projections in the monkey. An anterograde tracing study. Brain Res 1985;329:241–257.
27. Fudge JL, Kunishio K, Walsh P, et al. Amygdaloid projections to ventromedial striatal subterritories in the primate. Neuroscience 2002;110:257–275.
28. Friedman DP, Aggleton JP, Saunders RC. Comparison of hippocampal, amygdala, and perirhinal projections to the nucleus accumbens: combined anterograde and retrograde tracing study in the Macaque brain. J Comp Neurol 2002;450:345–365.
29. Kunishio K, Haber SN. Primate cingulostriatal projection: limbic striatal versus sensorimotor striatal input. J Comp Neurol 1994;350:337–356.
30. Schultz W. Multiple reward signals in the brain. Nat Rev Neurosci 2000;1:199–207.
31. Knutson B, Westdorp A, Kaiser E, Hommer D. FMRI visualization of brain activity during a monetary incentive delay task. Neuroimage 2000;12:20–27.
32. Breiter HC, Aharon I, Kahneman D, et al. Functional imaging of neural responses to expectancy and experience of monetary gains and losses. Neuron 2001;30:619–639.